Chapter 6
Design and Life Prediction

Shelf Life Failure Prediction Considerations for Irradiated Polypropylene Medical Devices

Michael T. K. Ling, Samuel Y. Ding, Atul Khare, and L. Woo
Baxter International, Round Lake, IL 60073, USA

INTRODUCTION

Ionizing sterilization is gaining popularity in medical device and packaging industry because of its convenience and lower cost. The mode of sterilization is a consequence of the high energy electrons released from the interaction of the gamma ray photons or electron beam particles with the materials being sterilized. These high energy electrons in turn interact with the DNA sequences in the microbiological burdens, through permanently altering their chemical structures to render them innocuous.

The high energy electrons, however, can also initiate ionization events in the material being sterilized. It can create peroxy and hydroperoxy free radicals in the presence of oxygen, and start the degradation cascade. This could result in an unacceptable color formation, excessive pH shifts and high extractable. Furthermore, the degradation could also lead polypropylene (PP) to well-publicized catastrophic failure during post radiation shelf life storage. From product quality and application viewpoints, it is thus highly desirable to develop a simple and rapid method to characterize the impact or most importantly the shelf life of radiation sterilized packaging materials or devices.

The purpose of this paper is to examine the various important parameters that need to be taken into consideration when a specific method is applied to predict the shelf life of a product made of polypropylene material.

EXPERIMENTAL

Technique used in this study includes ASTM D3895-92 isothermal oxidative induction time (OIT) from Dupont 1090 thermal analyzer with 910 differential scanning calorimetry (DSC) cell. OIT was conducted under air flow condition of 100 CC/min. The thickness is usually 5 mil or thinner. Failure morphology was examined by JEOL 35CF-SEM after sputter coating with palladium for surface conductivity.

RESULTS AND DISCUSSIONS

THE EFFECT OF LONG LIVED FREE RADIALS

Both the sterilizing action and the degradation caused by ionizing radiation are believed to result from Compton secondary electrons from the primary interaction event. The high energy gamma photons or accelerated electrons (from the e-Beam source) interact with the atoms in the material, creating a secondary high energy electron and a recoiling photons or electrons. These electrons can lead to a series of secondary ionization events in localized spurs. The cascade is propagated until all the excess energy above the ionization threshold is dissipated. Thus from a single incoming photon or electron, a binary tree configuration of secondary electrons are generated, and they are responsible for the bioburden kill and material degradation.

Catastrophic failures have been reported during the PP shelf life storage period. Intense investigation has come to the following hypothesis: Long lived free radicals trapped in the crystalline domains slowly migrate towards the crystalline /amorphous interface where they react with available oxygen to form peroxy and hydroperoxy radicals and initiate degradation near the interface. When sufficient number of the tie molecules between crystallites were cut through this chain scission process, PP elongation is reduced dramatically and catastrophic failures followed. At the same time, since the outer surface is more exposed to atmospheric oxygen, the extent of degradation near the surface is much greater than that of the interior. A brittle layer is then formed and has the same effect as forming sharp notches on the sample, creating stress concentrations. Once the notch reaches a critical size, failure occurs.

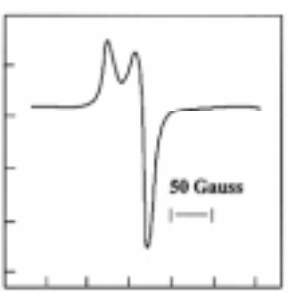

Figure 1. EPR signal of PP, 6 mo. post irradiation.

To confirm that long lived free radicals do play a significant role in the post irradiation PP degradation, a PP film sample was examined by electron paramagnetic resonance (EPR) spectroscopy at room temperature, Figure 1; the PP film was about 6 months old after an irradiation dose of 25 KGy dose at about 10 KGy/hr rate. It is seen that the free radical mediated oxidative deg-

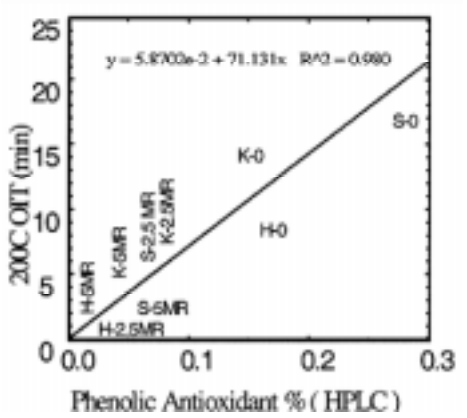

Figure 2. PP OIT vs. antioxidant concentration.

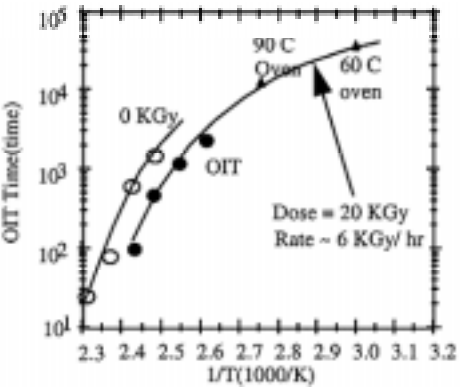

Figure 3. Combined Arrhenius plot of OIT data (DSC) and oven data (brittleness).

radation continues in polypropylenes long after the irradiation event. Incidentally, the strong EPR signal was completely eliminated when the sample was annealed in a vacuum oven at 90°C, a temperature much above the glass transition for the amorphous phase for PP, and well into the alpha relaxation for the crystalline phase of PP.

SHELF LIFE PREDICTION BY OIT (OXIDATIVE INDUCTION TIME) FOR PACKAGING FILMS

The remaining antioxidant in the PP material post irradiation is very critical to protect against further degradation. The action of the phenolic antioxidant is mainly that of a hydrogen donor in eliminating organic free radicals and becomes sacrificially consumed in the process; once it is completely consumed, catastrophic failure of PP will occur. Therefore, the ability to measure the remaining antioxidant is very useful for shelf life prediction. Confirming what have been widely reported in the literature,[1] we also found that, OIT at various temperatures was an excellent linear function of active antioxidant content, Figure 2. The exceptionally linear response of OIT at multiple temperatures strongly indicates the potential of using this method for simple and very rapid, although non-specific assay for active antioxidant determination.

OITs of a radiation copolymer PP film of about 5 mil in thickness was determined before and after 20 KGy of gamma exposure at about 6 KGy/hr dose rate. The data was plotted in the Arrhenius form in Figure 3. It is clearly seen that the gamma exposure has significantly reduced the OIT throughout the temperature range studied. To access stability at

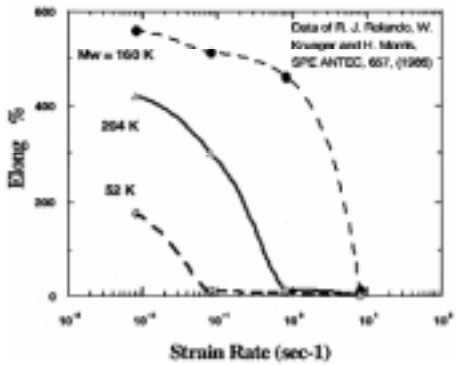

Figure 4. Strain rate effect on PP.

still lower temperatures, where the OIT detection becomes difficult, the gamma exposed films were subjected to oven aging at 90°C and 60°C. Their failure times were noted when film samples became brittle. Interestingly, when the oven failure data were plotted onto the Arrhenius plot with the gamma samples, a continuous curve with diminishing slope toward lower temperatures emerges. This kind of continuity of functional behavior of OIT data at higher temperatures and oven stability data closer to ambient could, at least in principle, produce long term property prediction based on OIT data, provided that the rate of slope change can be determined separately. It was observed that the slope of Log OIT vs. 1/T at any 1/T is nearly constant for many of the polypropylene tested regardless homopolymer or copolymer in nature or radiation history. For example, the 20KGy curve of Figure 3 can be shifted vertically by a single factor to coincide with the non-irradiated sample. This implies that if a "master curve" could be constructed, the shelf life of the PP can be predicted once the shift factor is determined. The determination of the shift factor should only involve a single, or at the most, a few carefully chosen calibration points.

A detailed evaluation of this technique including the applicability of the master curve is currently underway and results will be reported in the future.

SHELF LIFE PREDICTION CONSIDERATION FOR THICK DEVICE

For a typical packaging film which is relatively thin compared to device, shelf-life prediction using OIT method as mentioned above is quite satisfactory according to our opinion. However, for a device many times thicker, the ductility of the entire device greatly depends on the ductility of the surface even though the bulk of the core material is still very ductile, the geometry, and the strain rate involved during in use. If the surfaces were brittle and their thickness exceeded the critical thickness, failure is likely to occur.

A few methods have been reported for PP shelf life predictions:

1. Molecular weight equivalent method[3]
2. High surface area, high orientation acceleration test[3,4]
3. Variable Q10 and D&A techniques[5] based on bending angles

Typically, the three points bending flexural test under ASTM D-790 is specified for polypropylene device post radiation testing. Under ASTM D-790, a strain rate of 0.01 min^{-1} (or 0.00016 S^{-1}) is specified for the outer fiber. From Figure 4, one can see that all polypro-

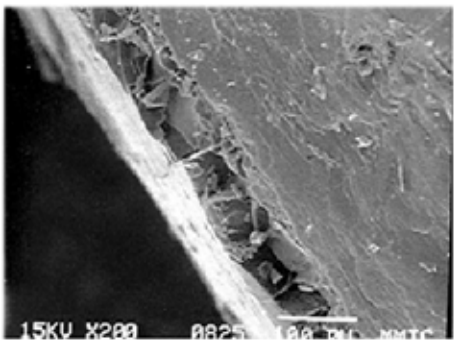

Figure 5. 15 year PP surface embrittlement.

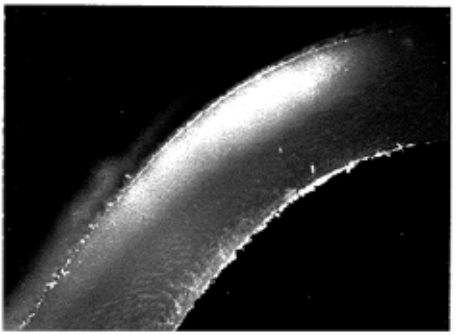

Figure 6. PP core, 15 yr. crazing, large strain.

pylenes regardless of molecular weight are quite tough. However, in an actual device application, significantly higher strain rates are encountered. For example, a suddenly loaded syringe flange is estimated to be subjected to a strain rate of about 0.5 sec^{-1} at the root. This is a factor of 3000 times higher than the ASTM bending test. In addition, strain rate at stress concentrated areas also shifted toward much higher levels. Based on the above discussion, strain rate, stress concentration factor (or geometry factor), molecular weight are all important factors that determine the ductility of the PP device. Knowing the brittleness dependency of strain rate, it is critical to chose the appropriate testing strain rate for an accurate shelf life prediction; too low the testing rate would lead to exceptionally high shelf lives and too high the testing rate would make all samples brittle. It is therefore extremely critical to determine the actual worst case strain rates to predict the shelf life of the device.

PP with an amorphous (T_g) of about 0^oC is not a tough material. Especially when subjected to high rates of strain, the glass transition is shifted to a higher temperature. The so-called ductile-brittle transition for PP is estimated to lie in the strain rate range of between 0.1 and 10 sec^{-1} at room temperature.[2] When the oxidative degradation progresses from the external surface, the fraction of the brittle layer steadily increases with time. The brittle layer has the same effect as forming surface notches, and the notches can shift the deformation to much higher strain rates. Hence, when a sufficient brittle layer has built up on the surface, even a slow deformation (strain) rate can have the same effect as a high rate event, catastrophic brittle failures becomes the inevitable outcome.

The growth rate of the brittle layer depends on the copolymer type and content of the PP, stabilizers package and morphology. Oxidation rate of semi-crystalline PP also depends on the degree of crystallinity. A gamma irradiated (50 KGy) PP copolymer (about 2 wt% ethylene) tensile bar was examined after 15 years of storage at ambient. A layer of surface embrittled polymer degradation product appears to cover the entire surface, while the core

of the sample remained relatively ductile. The scanning electron microscopy (SEM) morphology of a high speed fracture plane cross section, Figure 5, indicated about 100 micron thickness for the totally degraded layer; this is about 6.7 μm/year. When the brittle surface layer was removed, and the remaining interior sample subjected to a sharp bend of 180 degrees, very ductile behavior with massive crazing and stress induced whitening were observed, Figure 6. The formation of massive crazing in the stress whitening zone indicates that the mechanical behavior of the core material is near indistinguishable from that of un-irradiated polypropylene. From the core of the sample, the residual antioxidant content as assayed by the OIT, lies along the same trend line of un-aged samples. This indicated that the interior of the sample, where ambient oxygen could not diffuse in through the surface in sufficient quantities, 15 years post irradiation storage has little effect on the material property. This is a strong evidence that during post irradiation storage, the oxygen diffusion is the limiting factor for degradation, and the brittle behavior is mainly due to the brittle skin that form a notch and magnified the local stress and therefore the strain rate to cause a brittle failure.

Only a slight deformation is needed to cause the brittle surface to fracture to form cracks. These cracks act as sharp notches and the stress concentration factor depends on the radius of the crack tip. The stresses become infinite as the radius of the crack tip approaches zero; in this case a stress intensity function must be used to express the stress in the vicinity of the crack. For the propose of discussion, the notch is assumed to be blunt with a radius of r and a crack length of a, then the stress in the direction of the applied stress can be approximated by an elliptical solution and is expressed as[6]

$$\sigma = \sigma_0\left[1 + 2(a/r)^{\frac{1}{2}}\right] = \sigma_0 K_I \qquad [1]$$

Where K_I is the stress concentration factor and reduces to $K_I=2(a/r)^{1/2}$ for a relatively sharp notch($a>>r$). σ_0 is the applied stress at far field.

Notches not only introduce tri-axiality into the stress field, but also alter the strain rate in the highly stressed region around the root of the notch. The strain rates increase linearly with K_I or $(a/r)^{1/2}$ since strain is directly proportional to the stress for a linearly elastic material. The significance of strain rate on PP's ductility is seen in Figure 4.

From equation [1], one can see that with a steady increase in the notch depth, the stress concentration factor also increases. Hence, for a typical notch radius of 2 microns, these stress concentration factors are obtained.

Brittle Layer Thickness, (microns)	Stress Concentration Factor, K_I
1	2.4
10	5.5
100	15.1

It can be seen then, stress concentration factor of about 2 to 15 are encountered. This is also the factor based on linear elasticity which allow one to scale the local strain rate based on the brittle layer thickness. Using data from Figure 4, one can estimate the ductility for the sample or device. For example, for a 10 micron brittle layer thickness, or an acceleration of about 5, and a nominal strain rate of 0.5 sec^{-1}, both the low and high molecular weight samples are becoming brittle, while the medium molecular weight sample remains relatively unaffected. However, at a brittle layer thickness of 100 microns, or an acceleration factor of about 15, the medium molecular weight sample also lost its ductility completely.

With these parameters quantified, one can begin to construct a model for property prediction. In the case of near complete depletion of antioxidants, immediately after radiation one can factor the brittle layer advancing rate into the component thickness and the expected strain rate.during use, to arrive at a reasonable conclusion on storage shelf life at any temperature where ductile behavior can be maintained. As usual, all predictions based on theoretical considerations need to be validated with parallel real time aging studies.

SUMMARY

Factors governing polypropylene's post radiation shelf life to maintain the mechanical ductility were identified. The oxygen diffusion limited degradation model first proposed by Gillen and Clough[7] was experimentally confirmed. From a sample with 15 years of real time ambient aging, the advancing velocity of the surface embrittled zone was determined. It is proposed to incorporate the surface brittle layer thickness into an overall model based on stress concentration factor and the strain rate dependence for device and component shelf-life prediction.

An OIT method was found useful in determining the stability of PP at high temperatures, and the data may be extrapolated to ambient temperature to predict the shelf life of PP by following the curvature, non-Arrhenius behavior, of Figure 3.

REFERENCES

1 G. N. Foster, **Oxidation Inhibition in Organic Materials**, Vol.2, J. Pospisil, P. Klemchuk eds., *CRC Press*, Boca Raton (1989).
2 R.J. Rolando, W. Krueger and H. Morris, SPE Proceeding, ANTEC, 657, 1986.
3 L. Woo at al, Shelf Life Prediction Methods and Applicabilities, ANTEC '91, P1854.
4 L. Woo, C. Sandford, and R. Walters, in **Advances in Biomaterials**, P.52, Edited by S.M. Lee, *Technomic Publishing*, Lancaster, 1987.
5 Donohue, and S. Apostolou, Predicting Post-Rad Shelf Life from Accelerated Data: The D&A Process, "Technical papers, Brookfield, CT, SPE, 42:2819-2822, 1996.
6 J.G. Williams, **Stress Analysis of Polymers**, *Halsted Press, John Wiley& Sons*, NY, 1973.
7 K. Gillen and R. Clough, **Irradiation Effects on Polymers,** D. W. Clegg and A. A Collyer Eds. *Elsevier Applied Science,* New York, 1991.

Determining Etch Compensation Factors for Printed Circuit Boards

Anthony DeRose, Richard P. Theriault and Tim A. Osswald
Polymer Processing Research Group, University of Wisconsin-Madison, Madison, WI, USA
Jose M. Castro
Ohio State University, Columbus, Ohio, USA

STANDARD PROCESSING METHOD

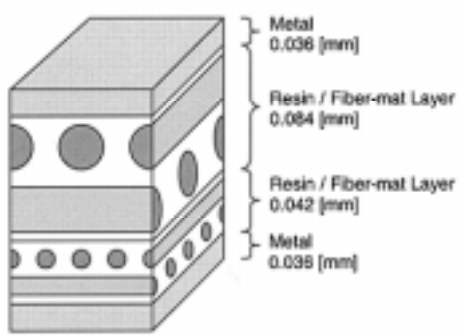

Figure 1. Schematic of metal-clad, multi-layered, fiber matrix reinforced thermoset laminate.

Metal-clad, multi-layered, fiber mat reinforced, thermoset resins are typically processed in either an autoclave or within a press. In either case, the individual plies are first sequentially layered, as depicted in Figure 1 and pressed as a stack, or book of laminates as shown in Figure 2. The book is then subjected to a mold temperature and pressure schedule to advance the degree of cure and adhere the plies to form the laminate composite. A typical mold temperature and pressure schedule for the pressing of laminate composites is illustrated in Figure 3.

In stage I of the processing schedule shown in Figure 3, the resin viscosity decreases due to the influence of the heat transfer from the molds and flow occurs upon the application of pressure. Stage II is characterized by the steady increase in the degree of cure. Since the mold temperature during stage II is higher than the glass transition temperature, T_g, of the resin, the residual stress developed due to curing strain and flow are in competition with the stress relaxation process within the polymer network. In the ideal case, it has been found that residual stress is completely relaxed by the time the material is cooled below T_g.[1] The pressure profile during stage II is maintained at a high level to impede the growth of voids which may exist within the resin. The mold temperature profile associated with stage III is typically a crash, or sudden cooling, of the laminate through the T_g of the resin. The cycle terminates when the laminate can be eas-

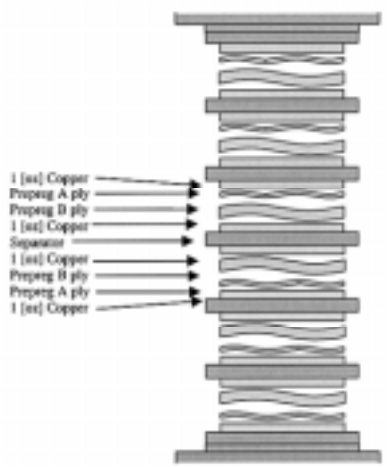

Figure 2. Schematic representation of ply sequence within a six laminate book.

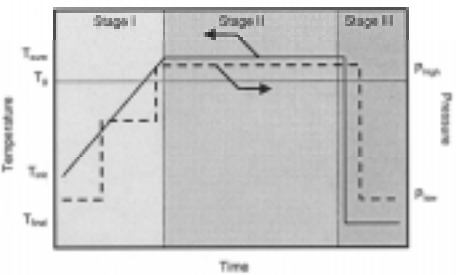

Figure 3. Platen temperature and pressure scheduling.

ily handled and removed from the press. Optimization of this time period will lead to the minimization of the processing induced stress.

Once the laminates are removed from the press the circuit patterns are developed by chemically removing the unwanted metal from either side of the laminate. During this operation much of the residual stresses that have developed within the metal layers are transferred to the thermoset layers. The cured and etched laminates can then be sandwiched between prepregs and restacked in the mold. Repeating this cycle leads to the production of multi-layered circuit boards.

MODEL DEVELOPMENT

CURE KINETICS

The conversion of a thermoset to a glassy solid involves two transitions: gelation and vitrification. Gelation is the time at which covalent bonds form to generate a three-dimensional network that gives rise to long range elastic behavior. Vitrification is when T_g of the system rises to the cure temperature and when further reaction is prohibited or is dramatically reduced.

The degree of cure can be assumed to be proportional to the number of bonds formed during crosslinking such that each bond releases the same amount of heat. Thus, the degree of cure can be defined as

$$c = \frac{Q}{Q_T} \qquad [1]$$

where Q_T is the total heat of reaction and Q is the amount of heat released up to the current time. The rate of heat generation can be expressed as

$$\dot{Q} = Q_T \frac{dc}{dt} \quad [2]$$

where the cure rate term can be described using an empirical model. One such model is the Kamal-Sourour[2] reaction model written as

$$\frac{dc}{dt} = (k_1 + k_2 c^m)(1 - c)^n \quad [3]$$

where k_1 and k_2 are kinetic rate constants, and both m and n describe the reaction order. The kinetic rate constants have been modified by the Rabinowitch model[3] as suggested by Havlicek and Dusek,[4] to account for the diffusion of the chain segments as

$$\frac{1}{k_i} = \frac{1}{k_{i,c}} + \frac{1}{k_d} \quad [4]$$

where $k_{i,c}$ is the Arrhenius kinetic rate constants for both *1* and *2* and k_d is the Arrhenius kinetic rate constant for the diffusive effects described by

$$k_d = a_d \exp\left(\frac{-E_d}{RT}\right) \exp\left(\frac{-b}{f}\right) \quad [5]$$

where a and b terms are rate constants, E_d are activation energies, f accounts for the equilibrium fractional free volume, R is the gas constant and T is the temperature.

When the T_g of the material rises beyond the cure temperature, i.e., after vitrification, diffusion becomes the dominating mode of transport.

The ability to predict the point of gelation and T_g is important in being able to predict the formation of residual stress. At the point of gelation, a network of crosslinked chains propagates throughout the resin, thus enabling the semi-solid resin to withstand stress.[5] A statistical approach to predict the degree of cure in which the resin can withstand residual stress is proposed by Flory's theory of gelation.[3] For example, a stoichiometric mixture of DGEBA and a tetra-functional aromatic amine would yield a theoretical conversion at gelation of 0.57.[7] Predicting the progression of T_g is important in determining the point where residual stress development during cooling is initiated. For a system exhibiting a one-to-one relationship between T_g and conversion, DiBenedetto's equation[8] is an approach for stoichiometric ratios to express this relationship using only a single parameter model.

In order to solve the kinetic models aforementioned, we must first solve the transient heat transfer from the mold to the laminate. The governing equation for heat transfer is the energy balance for heat conduction expressed as

$$\rho C_p \frac{\partial T}{\partial t} = k \nabla^2 T + \rho \dot{Q} \quad [6]$$

This equation can be reduced to one-dimension assuming that the planar heat transfer through the laminate can be neglected compared to the through thickness temperature transients. Laminates are typically thin enough such that the exothermic heat generated due to

conversion can be conducted out of the resin relatively quickly, and therefore, the source term, $\dot{Q}$, can be neglected. The Crank-Nicolson Method was used to approximate Eq. [6] which results in a system of equations that can be solved using the Thomas Algorithm.[9]

MECHANICAL PROPERTIES

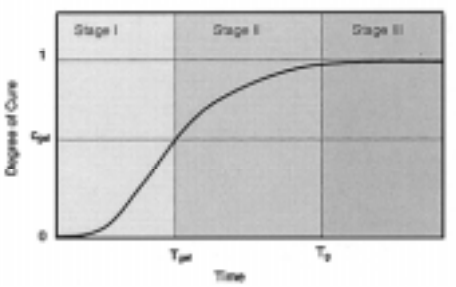

Figure 4. Conceptual model for the progression of cure of thermoset resins.

As a thermoset cures, the mechanical properties of the material behave similar to a viscous liquid in its uncured state and similar to an elastic solid in its fully cured state. It is convenient to divide the curing into three stages, as shown in Figure 4. In Stage I the material is considered a viscous fluid, with negligible stiffness. In Stage II, conversion has advanced to form a network gel and the mechanical properties, such as the stiffness, develop. The progression of the elastic modulus during this stage has been reported to have a linear relationship with the degree of cure.[10] Stage III indicates that the degree of cure of the material has reached a terminally high value.

For epoxy resin systems it has been found that the curing strain due to conversion can be neglected in the residual stress analysis.[5] For laminate composites, the CTE (coefficient of thermal expansion) of the plies, non-uniform cooling, and the removal of the copper during the etching stage of the process significantly influences the residual stress profile leading to dimensional movement.[11] Thus, the factors that dominate the residual stress profile are the mechanical properties of the individual plies at the point of cool down.

To evaluate the dimensional movement of the laminate, the generalized Classical Lamination Theory was implemented.[12] This theory allows for the prediction of the thermal residual stress as a function of the complex coupling effects associated with planar movement and warpage. The generalized theory for stress takes the form

$$\{\sigma\}_k = [\bar{Q}]_k(\{\varepsilon^0\} + z\{\kappa\} - \{\beta\}_k \Delta T_k) \qquad [7]$$

where $\{\sigma\}$ is the stress, $[\overline{Q}]$ is the reduced stiffness matrix, $\{\beta\}$ is the CTE and ΔT is the temperature difference at the k^{th} laminate. The dimensional movement of the laminate is associated with mid-plane strain, $\{\varepsilon^0\}$, and the mid-plane curvature, $\{\kappa\}$.

The additional movement that occurs during the etching process is a result of the transfer of residual stress from the metal layers to the reinforced thermoset as the metal is chemically removed. Using the predicted residual stress profile in the first half of the simulation, we can determine how much of this stress is removed as a function of the metal removed during etching. The subsequent strains that result from removing this portion of the residual

stresses can then be calculated. This method allows us to specify the amount of metal that is removed in either of the planer directions for each side of a laminate independently. Etch compensation factors are then developed for each laminate based on the total predicted shrinkage. These etch compensation factors can then be used as a factor by which the artwork should be magnified to take into account the final amount of shrinkage the laminate will undergo during processing. This will insure that each layer of circuits will align as expected within the final board. The etch compensation factors in the warp and fill direction for the k^{th} laminate can be expressed symbolically as

$$f_k^W = 1 + \varepsilon^W{}_k \quad [8]$$

$$f_k^F = 1 + \varepsilon_k^F \quad [9]$$

where ε_k^W and ε_k^F are the predicted total strains in the warp and fill directions of the k^{th} laminate, respectively.

NUMERICAL PREDICTION

The simulation was used to analyze an unsymmetric laminate similar in construction to the diagram shown in Figure 1. The general laminate construction is shown in Table 1, and the more specific mechanical properties of the individual components of this laminate are shown in Table 2.

Table 1. Prepreg laminate construction and properties.

	Prepreg A	**Prepreg B**	**Units**
Resin	Epoxy	Epoxy	-
Resin mass percent	63	52	%
Init. degree of cure	28	28	%
Mat Weave	Plain	Plain	-
Warp fibers	1800	450	m/kg
Fill fibers	1800	900	m/kg
Thickness	0.043	0.086	mm

The laminate was first examined at the stage in the process after removal from the press cycle, prior to the etching process. The residual stress profiles in both the warp and fill directions are shown in Figure 5. The total movement in the warp direction was 0.00232

[mm/mm] with a radius of curvature of 1550 [mm] towards Prepreg A. In the fill direction, the total movement was 0.00257 [mm/mm] with a radius of curvature of 2245 [mm] toward Prepreg B. Since the radius of curvature was smaller in the warp direction than in the fill direction the dominant mode of warpage was in the direction toward Prepreg A.

Table 2. Properties of individual plies.

Material	Property	Value	Units
Metal	Thickness	0.036	mm
	Density	8950.0	kg/m^3
	Thermal cond.	386.0	J/(s m K)
	Specific heat	385.0	J/(kg K)
	Thermal exp. coef.	16.5e-6	1/K
	Elastic modulus	110.0	GPa
	Shear modulus	40.0	GPa
	Poisson's ratio	0.355	-
Prepreg A	Thickness	0.042	mm
	Resin mass ratio	0.63	%
	Glass (warp/fill)	1.0	-
	Density	1538.8	kg/m^3
	Thermal cond.	0.17	J/(s m K)
	Specific heat	116.0	J/(kg K)
	Exp. coef. (warp)	18.2e-6	1/K
	Exp. coef. (fill)	18.2e-6	1/K
	E-Modulus (warp)	14.03	GPa
	E-Modulus (fill)	14.03	GPa
	Shear modulus	4.64	GPa

Table 2. Properties of individual plies.

Material	Property	Value	Units
Prepreg A	Poisson's ratio	0.32	-
Prepreg B	Thickness	0.084	mm
	Resin mass ratio	0.52	%
	Glass (warp/fill)	2.0	-
	Density	1669.9	kg/m^3
	Thermal cond.	0.20	J/(s m K)
	Specific heat	150.2	J/(kg K)
	Exp. coef. (warp)	11.3e-6	1/K
	Exp. coef. (fill)	24.0e-6	1/K
	E-Modulus (warp)	21.90	GPa
	E-Modulus (fill)	13.54	GPa
	Shear modulus	5.41	GPa
	Poisson's ratio	0.31	-

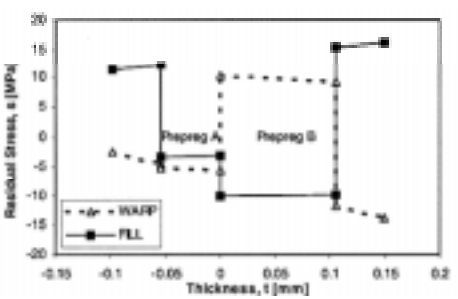

Figure 5. Stress profile of the unetched laminate.

Because we want to be able to calculate the movement of etched laminates in order to compensate the artwork, the analysis was repeated with the simulation of the etching stage incorporated.

A typical circuit pattern is shown in Figure 6. From this photograph the distribution of the remaining metal on the laminate was determined, which was then used in the simulation. This distribution is shown in Figure 7, and shows that approximately 3.2 percent of the circuitry runs in the warp direction (180 degrees), while approximately 2.4 percent runs in the fill direction (90 degrees) on either side of the laminate. Figures 8 and 9 show the additional

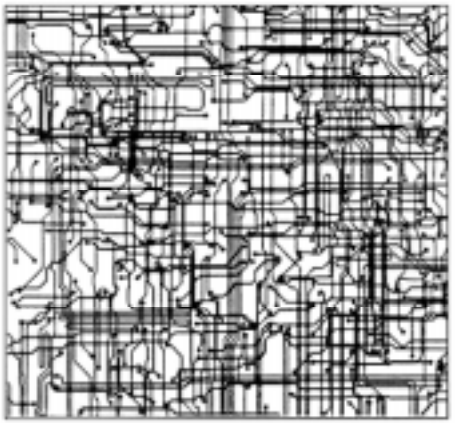

Figure 6. Photograph of the circuit pattern on a single laminate (both sides shown).

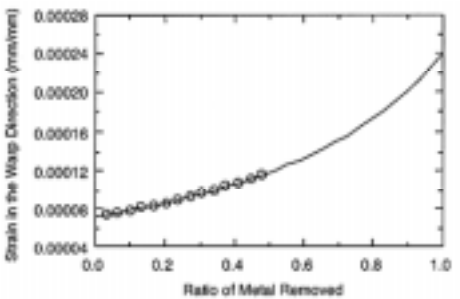

Figure 8. Predicted movement in the warp direction as metal is progressively removed (97.6 percent of metal was removed from fill direction initially).

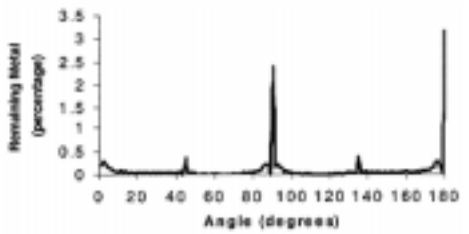

Figure 7. Circuit orientation distribution on laminate (180 is warp direction, 90 is fill direction).

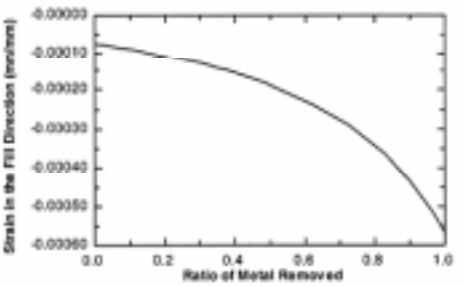

Figure 9. Predicted movement in the fill direction as metal is progressively removed (96.8 percent of metal was removed from the warp direction initially).

movement resulting from including the etching process in the simulation as a function of the amount of metal removed in the warp and fill directions, respectively. These additional strains are a result of the changing laminate equilibrium as the constraint of the metal is progressively removed. It is these values of strain that we then use to compute the etch compensation factors by which the artwork can be compensated. For example, Figure 8 shows that depending on the amount of metal removed in the warp direction during etching, the resulting movement in the warp direction can be as large as 0.8 mils per 10 cm of laminate. Subsequently, Figure 9 shows that etching metal in the fill direction can result in a movement of approximately 2.0 mils per 10 cm of laminate, or about twice the shrinkage for similar conditions as in the warp direction. As circuit patterns continue to decrease in size quantifying these movements will become important in reducing the number of circuit board failures.

CONCLUSIONS

Based on the nature of the process and the materials involved in the manufacturing of thermoset laminates it is difficult to avoid dimensional movement. This movement can result in the failure of circuit boards due to the misalignment of the circuitry on the various layers of the board. Simulation is perhaps the least expensive method for determining what this movement will be before the circuits are etched such that compensation factors can be applied in order to avoid these failures.

To increase the accuracy of these compensation factors, the model should be extended to capture the influence of the resin flow during the early stages of the process.

ACKNOWLEDGMENTS

The authors would like to gratefully acknowledge Allied Signal Laminate Systems, Inc, and the State of Wisconsin, Office of University-Industry Research for their support.

REFERENCES

1 Ochi, M., K. Yamashita and M. Shimbo, *J. Appl. Polym. Sci*., **43**, p.2013, (1991).
2 Kamal, M. R. and S. Sourour, *Polym. Eng. Sci.,* **13** (1), p.59, (1973).
3 Rabinowitch, E. *Trans. Faraday Soc*., **33**, p.1225, (1937).
4 Havlicek, I. and K. Dusek, in **Crosslinked Epoxies**, B. Sedlacek and J. Hahovec, eds., *Walter de Gruyter*, New York, (1987).
5 Wang, H.-B., Y.-G. Yang, H.-Y. Yu and W.-M. Sun, *Polym. Eng. Sci*., **35**, p.23, (1995).
6 Flory, P. J. in **Principles of Polymer Chemistry**, *Cornell University Press*, Ithaca, New York, (1953).
7 Riccardi, C. C., H. E. Adabbo and R. J. J. Williams, *J. Appl. Polym. Sci*., **29**, (1984).
8 DiBenedetto, A. T. *J. Polym. Sci. Polym. Phys*., **25**, p.1949, (1987).
9 Stikwerda, J. C., in **Finite Difference Schemes and Partial Differential Equations**, *Wadsworth & Brooks/Cole*, California, (1989).
10 Kim, K. S. and H. T. Hahn, *Comp. Sci. Tech*., **36**, p.121, (1989).
11 Brahatheeswaran, C and V. B. Gupta, *Polymer*, **34** (2), p.289, (1993).
12 Gibson, R. F. in **Principles of Composite Material Mechanics**, *McGraw-Hill*, New York, (1994).
13 Karkanas, P. I., I. K. Partridge and D. Atwood, *Polym. Int*., **41**, p.183, (1996).

Activation Energies of Polymer Degradation

Samuel Ding, Michael T. K. Ling, Atul Khare and Lecon Woo
Baxter Healthcare, Round Lake, IL 60073, USA

INTRODUCTION

In the study of polymer degradation and durability, there is little reliable, predictive methodology that is universally valid over wide spans of temperature and time. Many of the high temperature "accelerated" oven tests have been deemed unrealistic for different mechanisms were prevalent. In the mean time, for practical reasons, experimental time spans of much longer than a year are extremely difficult to conduct.

In the medical plastics industry, products are frequently sterilized by ionizing radiation, which severely depletes the antioxidant package. Yet to conform to many regulatory requirements, a scientifically based estimate of post irradiation shelf life must be provided. Thus a better understanding on the time and temperature influence on the material's performance is a necessity for product introduction.

In this study we have examined the Arrhenius activation energy as a function of temperature for many polymer systems important in the medical industry. Data from oxidative induction time (OIT), accelerated oven aging, and real time ambient storage to up to 23 years will be used to determine the functional behavior and quantitative significance of the activation energy.

EXPERIMENTAL AND MATERIALS

Technique used in this study includes ASTM D3895-92 isothermal OIT from Dupont 1090 thermal analyzer with 910 differential scanning calorimetry (DSC) cell. Forced convection air circulating ovens were used at various temperatures to assess long-term oven age shelf life with sample embrittlement as end points.

Morphological studies were done using a Reichert FC4E cryo-ultramicrotome to prepare undistorted material blocks for SEM analysis. SEM analysis was done with the JEOL 35CF-SEM after sputter coating with palladium for surface conductivity. In addition, other available characterization data were incorporated into this study.

The materials studied consist of polypropylene (PP), high density polyethylene (HDPE), low density polyethylene (LDPE), EPDM and polyester thermoplastic elastomers.

Gamma exposure at various doses was conducted in a laboratory gamma cell at dose rates of approximately 6-10 KGy/hr.

RESULTS AND DISCUSSION

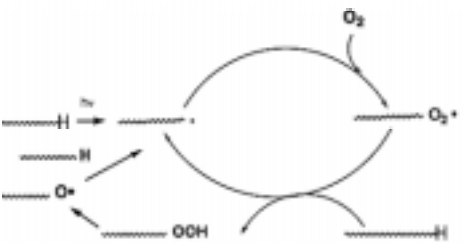

Figure 1. Oxidative kinetic chain reaction.

Both the OIT and chemo-luminescence data support the general mechanism of degradation where the primary alkyl free radicals are propagated through atmospheric oxygen diffusing into the polymer via the formation of peroxy and hydroperoxy free radicals (Figure 1). The rate limiting steps in this complex chain reaction scheme determine the overall degradation rate. In this regard, the action of stabilizer, such as phenolic antioxidants, chocks a section of the degradation loop by eliminating organic free radicals, or decomposing the hydro-peroxides, and becomes.sacrificially consumed in the process. The activation energy of the degradation rate, as expressed in the Arrhenius form, will be affected by factors such as polymer composition, stabilizer package, and polymer morphology.

GAMMA RADIATED POLYPROPYLENE

Catastrophic failures have been reported during the PP shelf life storage period. Intense investigation has come to the following hypothesis, that, long lived free radicals trapped in the crystalline domains slowly migrate towards the crystalline /amorphous interface where they react with available oxygen to form peroxy and hydroperoxy radicals and initiate degradation near the interface.[1,2] When sufficient number of the tie molecules between crystallites were cut through this chain scission process, PP's elongation is reduced dramatically and catastrophic failures followed.

To establish that long lived free radicals do play a significant role in the post irradiation PP degradation, a PP film sample was examined by electron paramagnetic resonance (EPR) spectroscopy. A distinct free radical spectrum was detected at room temperature about 6 months after irradiation. Incidentally, the strong EPR signal was completely eliminated when the sample was annealed in a vacuum oven at 90^{o}C, a temperature much above the glass transition for the amorphous phase for PP, and well into the alpha relaxation for the crystalline phase of PP.[3]

In a separate study, a radiation grade PP's OIT under air flow conditions of 100 ml/min was determined and the result compared with the same film sample (about 130 micron in thickness) after 20 KGy of gamma exposure at about 6 KGy/hr dose rate. To access lower

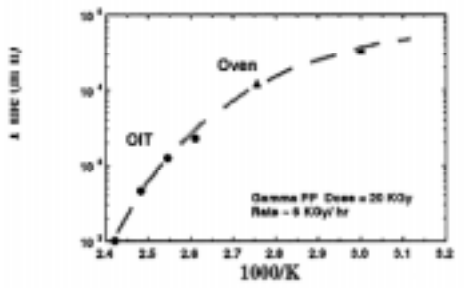

Figure 2. Combined Arrhenius plot of OIT and oven times for gamma irradiated PP.

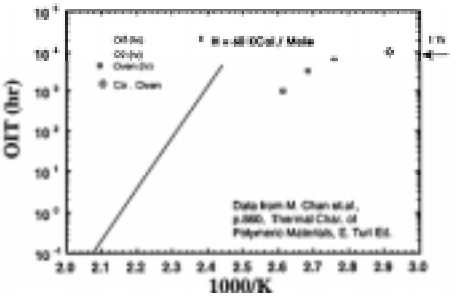

Figure 3. Bell Lab OIT and oven aging data on LDPE cable compound.

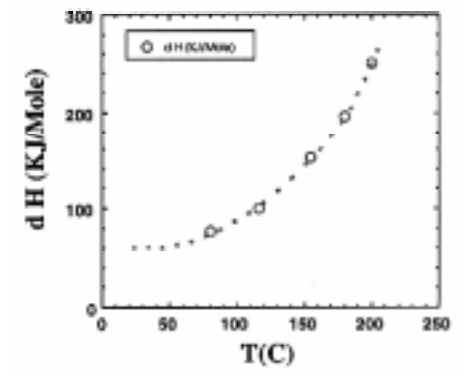

Figure 4. LDPE cable activation energies.

temperatures thermal stability, where the OIT detection becomes difficult, the gamma-exposed films were subjected to oven aging at 90 and 60^{o}C and their failure times noted. When the OIT and oven failure times were plotted onto the Arrhenius plot for the gamma irradiated samples, a continuous curve with diminishing slope toward lower temperatures emerges (Figure 2). This kind of continuity of functional behavior of OIT data at higher temperatures and oven stability data closer to ambient could, at least in principle, produce long term property prediction based on OIT data, provided that the rate of slope change can be determined separately. Further experiments along this line of reasoning are being carried out currently to explore the boundary of validity for several polymer systems.

LOW DENSITY POLYETHYLENE

This continuous curve behavior was very reminiscent of the data on crosslinked low-density polyethylene cable compounds studied with OIT, oxygen uptake, and oven aging experiments at the former Bell Telephone Laboratories,[4] (Figure 3). When the high temperature results were extrapolated by the Arrhenius equation to lower temperatures, grossly and physically impossible optimistic results were obtained. An examination of the activation energies indicated a more than four-fold difference between the high temperatures and near ambient (Figure 4). This observation prompted the Bell lab researchers cautioning against using the high temperature OIT for low temperature durability predictions. Nevertheless, by

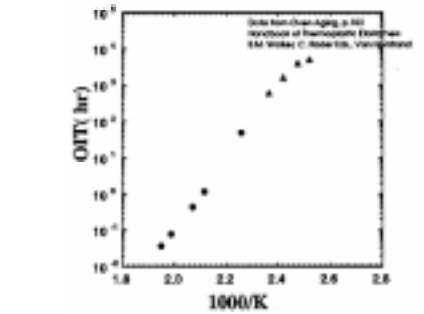

Figure 5. EPDM rubber OIT and oven aging.

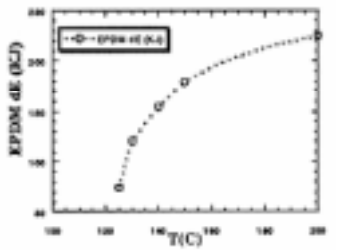

Figure 6. EPDM activation energies.

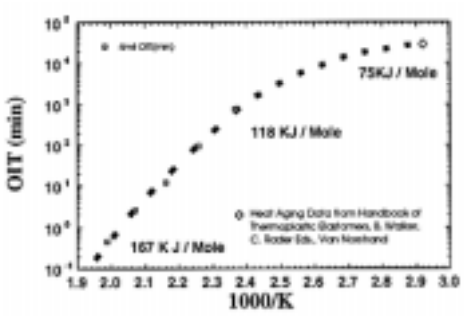

Figure 7. OIT of polyester thermoplastic elastomer.

recognizing the curved nature of the durability function, one can indeed achieve realistic predictions.

EPDM RUBBER

A new class of thermoplastic elastomers was created when olefinic polymers (polyethylene, polypropylene) are dynamically vulcanized with a crosslinkable elastomer such as ethylene propylene diene rubber (EPDM). These so-called thermoplastic vulcanizes are quite resistant to oxidation and studies have been available on their stability over long period of time.[5] A general-purpose thermoplastic sample of 50 Shore D hardness was chosen for the OIT study. Published data from a long term oven aging study for 50% strength reduction was plotted on the same graph for comparison (Figure 5). The activation energies at several temperatures are plotted in Figure 6.

POLYESTER ELASTOMER

Polyester thermoplastic elastomers (TPE) based on polybutylene terephthalate (PBT) hard segment and tetramethylene ether (PTMO) soft segments constitute an important class of medical elastomers because of their wide property range, solvent bonding capability, oxidative stability and processing ease. OIT measurements conducted in air at higher temperatures again coincided with the oven aging data reported in the literature (Figure 7). The activation energies at several temperatures are also calculated.

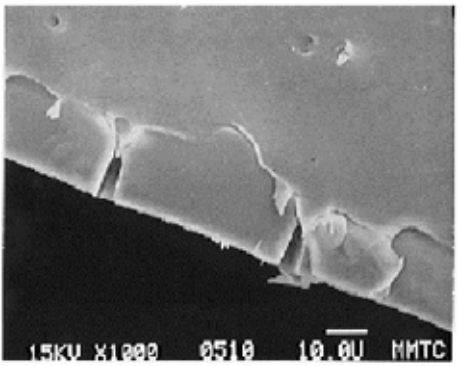

Figure 8. PP surface "fibrils" at 60X.

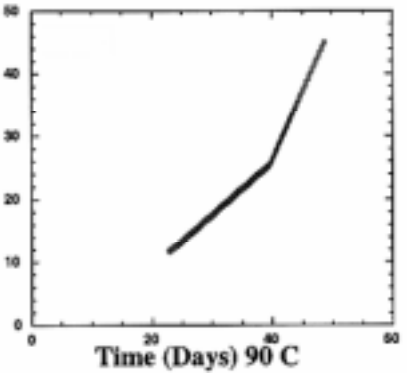

Figure 9. PP crack depth in microns.

PP SURFACE EMBRITTLEMENT

For an electron beam irradiated PP film sample undergone oven aging at 90^{o}C, a curious phenomenon was observed. About 3 weeks into oven aging, surface fibrils orthogonal to the exposed film edge surface became visually observable. Under optical and electron microscopic observation, these fibrils are showed to be shallow, surface cracks (Figure 8). These cracks appeared to grow in number and their depth (measured in cross section by SEM) increases linearly as a function of time. The linear crack depth growth significant accelerated at approximately 25% of the film thickness (or about 50% of the film volume) (Figure 9). The activation energies determined from the rate of surface embrittlement are:

Temperature, ^{o}C	30	70	90
E_a, kJ/mole	16	41	82

PP ACTIVATION ENERGY FROM OIT, OVEN AGING AND REAL TIME AGING

Recently, in the authors' laboratories, several prototype and production polypropylene bottles, which have been stored under ambient conditions for up to 23 years, were discovered. This "find" could allow the calibration of our long-term durability prediction methods. When the OIT of these products were determined, an excellent linear relationship with storage time, pointing to the zero OIT time of about 30 years. Hence, we can state, with reasonable assurance, that the durability of this particular grade of PP in the thin film form, under ambient storage, is about 30 years. When this data was combined with newly generated OIT and oven life data, plotted in the Arrhenius form, a continuous curve covering nearly 8 decades (100 million folds) of time was obtained (Figure 11). And when the local slopes

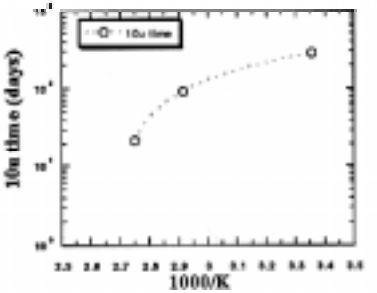

Figure 10. Rate of degraded layer formation.

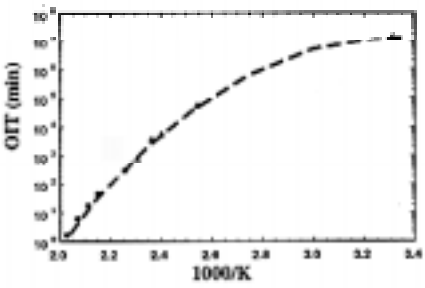

Figure 11. Combined OIT, oven aging and real time aging data of PP.

were measured and converted to the activation energy at various temperatures, again, a concave curve resulted.

Yet another significant observation on PP is that the activation energy from thermal aging processes when compared with the activation energies of the rate of brittle layer formation, near identical results are obtained. This apparent " self-similarity ", or near identical activation energies at the same temperature exhibited for different degradation measurement parameters and different grades of polypropylene, could lead to much simplified modeling and understanding of the degradation and durability process. Efforts are currently underway to gather more supporting data on this self-similarity and the utility it could bring.

SUMMARY

A broad based study on the kinetics of polymer degradation was conducted. The Arrhenius activation energy was used as the parameter to follow the rate dependence with temperature. For most systems, a monotonic increasing trend with temperature was evident. This finding explains the frequent observation that kinetic parameters obtained at high temperatures often lead to grossly optimistic results at ambient. For a polypropylene copolymer system, combined data from OIT, oven aging and real time storage of up to 23 years, yielded one of the most complete data sets covering over 8 decades of time. When the activation energies from thermal processes were compared with the rate of surface embrittlement, a striking self similarity, or near identical activation energies at the same temperature were evident. This observation could lead to broader applications and further understandings on the polymer degradation.

REFERENCES

1. G. N. Foster, in **Oxidation Inhibition in Organic Materials**, Vol.2, J. Pospisil, P. Klemchuk eds., *CRC Press*, Boca Raton (1989).

2. L. Matisova-Rychla and J. Rychly, in **Polymer Durability**, R. Clough, N. Billingham, and K. Gillen Eds, *Am. Chem. Soc*., Washington, DC (1996).
3. L. Woo, J. Palomo, T.K. Ling, E. Chan, C. Sandford, *Medical Plastics and Biomaterials*, **3**, (2), 36 (1996).
4. H. E. Bair, **Thermal Characterization of Polymeric Materials**, p. 869, E. Turi Ed., *Academic Press*, New York, (1981).
5. N. R. Legge, G. Holden, and H. E. Schroeder, eds, **Thermoplastic Elastomers**, *Hanser MacMillan*, New York, (1987).

Estimation of Time-temperature-collectives at Describing Ageing of Polymer Materials

D. Blaese and E. Schmachtenberg
University of Essen, Institute for Plastics in Mechanical Engineering (IKM), Altendorfer Str. 3, 45127 Essen, Germany

INTRODUCTION

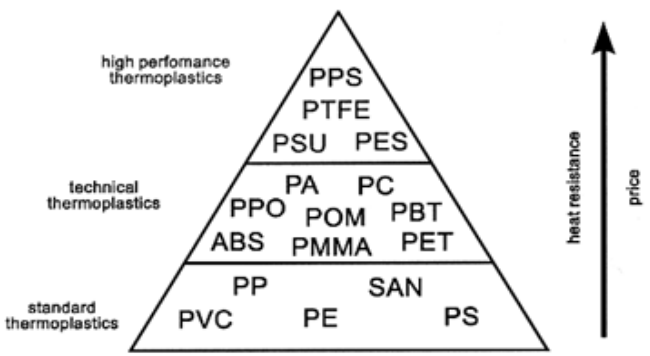

Figure 1. Classification of thermoplastic materials.

The development of innovative products by using plastic materials represents a great challenge in respect to the material selection for the new product. The selection of a suitable material for a given application is not only influenced by the construction of the product and the processing of the material but also essentially influenced by the operating conditions of the product.

One problem at the material selection is the large number of different obtainable plastic materials. Only for thermoplastic materials more than 10,000 trading products are available. The prices for these materials differ between 1 $/kg (e.g. PE) and 100 $/kg (e.g. PAEK). Closely associated with these costs for the raw material the properties of these plastic materials are very different. One example for this connection between price and property of a material is illustrated in Figure 1 for the property of heat resistance.

This connection shows that the production costs of technical products of plastic materials are the main reasons for a systematic material selection. An evaluation of the production costs for an exemplary product which is produced by the injection molding process the costs of the material amounts to 55% of the production costs (Figure 2). This percentage of the material cost depends on the applied material and also on the output of the product.

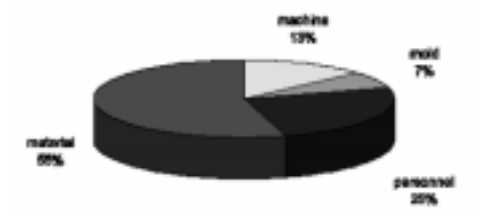

Figure 2. Production costs (example: injection molding, polyamide, weight 190 g, 180,000 pieces a year).

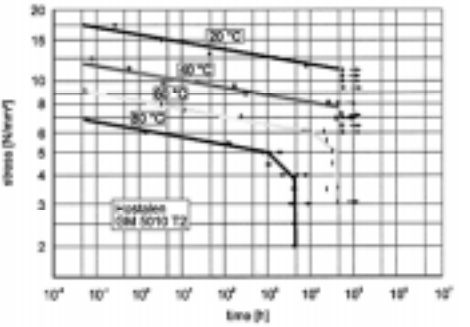

Figure 3. Decrease of strength vs. time for polyethylene-pipe.

This points out that a systematic material selection is essentially important for the economic production of plastic products as well as for the suitability for the application.

Furthermore plastic materials age under operating conditions. The loading of a product for example is given by the influence of a medium, a temperature and also a mechanical loading. Figure 3 shows the decrease of strength of polyethylene pipes. In this figure three different sections with three different gradients can be distinguished. The reason for these sections are the three different damaging processes of polyethylene by loading under temperature and a medium.

This causes that the ageing of a plastic material is essentially influencing the lifetime of a product. Because of this it can be shown that the ageing and lifetime of a product is an essential aspect in the course of the material selection which has to be taken into consideration.

Especially the influence of a medium can cause different interactions with the material and combined with this the influence of a medium effects different failure mechanisms of the product.

It has to be taken into consideration that the different mechanisms cannot be analyzed separately. On the contrary to this a superposition of these effects is the result and they are influencing each other.

But how to analyze the lifetime of a product and the suitability of the material for the given application after preselection of a plastic material?

TIME-TEMPERATURE-EXTRAPOLATION WITH ARRHENIUS

Generally such an estimation of lifetime can be conducted by suitable and praxis relevant product tests. Hereby it has to be guaranteed that the complexity of the application also can be reproduced in the product test. It is very important for the concept of these tests that a characteristic product value can be measured. This characteristic product value represents a

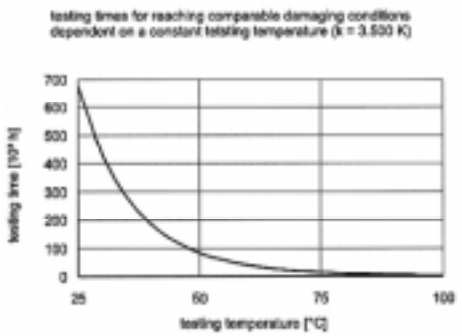

Figure 4. Time-temperature-shifting-principle.

scale for the damaging of the product and depends on the loading of the product.

In practice a method is established which estimates the limits of application by time-temperature-extrapolation of the measured damaging processes. So a lifetime prediction is possible by using the time-temperature-shifting-principle (Figure 4).

This time-temperature-shifting-principle says that the influence of a high temperature for a short time causes a comparable damaging as a low temperature for a long time.

One possibility to describe the time-temperature-shifting is given by the statement of Arrhenius. This is shown in equation 1:

$$\frac{t}{t_{ref}} = 10^{k\left(\frac{1}{T}-\frac{1}{T_{ref}}\right)} \qquad [1]$$

In this statement t stands for the required lifetime at a temperature T and t_{ref} stands for the testing time at the testing temperature, T_{ref}. Thereby the shifting factor k is the only unknown. This factor contains the influences of the used material, the given operating conditions like the medium and the loading as well as the influence of the construction.

The determination of the shifting factor k can be determined by the described product tests. For at least two different temperatures at different testing times products has to be taken from the test stand and the characteristic product value has to be determined. For two different temperatures two products are inspected which show an identical damaging according to the measured characteristic product value. This is equivalent for an identical damaging of the product in account of the ageing of the material.

With these two pairs of values with the following equation 2 the shifting factor k can be determined.

$$k = \frac{\log\left(\frac{t_1}{t_2}\right)}{\left(\frac{1}{T_1}-\frac{1}{T_2}\right)} \qquad [2]$$

With the determined shifting factor k the time-temperature-shifting can be calibrated for a given application. This shifting factor k is only valid for the given application, the used material and the examined product. A transfer to other products is only limited possible because of these reasons.

By using the statement of Arrhenius for time-temperature-shifting it has to be noticed that this statement is only valid in certain limits. These limits are given by the equilibrium temperatures of the plastic materials as the melting temperature or the glass transition temperature. Beyond it an extrapolation should not be conducted over a too large temperature range. The insecurity of the results increases with increasing difference between testing temperature and operating temperature.

ESTIMATION OF TIME-TEMPERATURE-COLLECTIVES

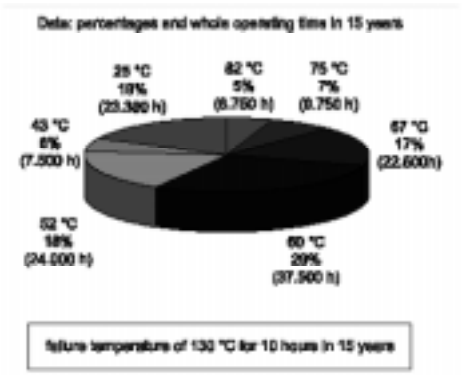

Figure 5. Time-temperature-profile.

In practice a loading under a constant temperature for the whole lifetime is not realistic. On the contrary a complex time-temperature-profile is given (Figure 5).

In this case it is possible to suppose the highest temperature for the whole lifetime as the critical temperature for the strength of the product. This leads to a high demand on the properties of the used material. So this procedure leads to a large over-dimensioning of the product and combined with this to a very uneconomic solution of the product idea.

A second way to consider such time-temperature-profiles is given by an estimation of the separate time-temperature-collectives with regard to their contribution of ageing. For this the following procedure is imaginable:

1. An "influence" is defined as a specified time-interval during which a specified medium with a constant temperature and under a constant loading is influencing the product.

2. This influence effects an "ageing" of the product. Different influences can be taken into consideration for the determination of ageing of the product by addition of the different parts. So an "ageing progress" is given by an influence.

3. If the ageing is advanced to a critical state the product changes its properties (e.g. decrease of strength, change of the molecular structure of the product or other).

4. The estimation of the different parts of ageing caused by an influence is conducted with the help of the time-temperature-shifting-principle.

For each influence a reference-time would be calculated which causes a comparable ageing progress at reference temperature. By addition of the separate reference times a total testing time for the product can be evaluated. This testing time at reference temperature

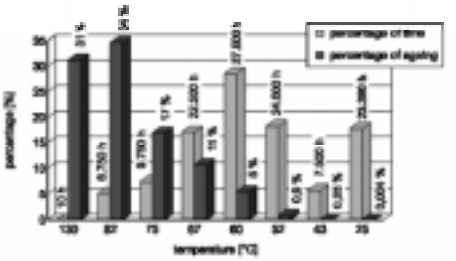

Figure 6. Percentages of time and ageing.

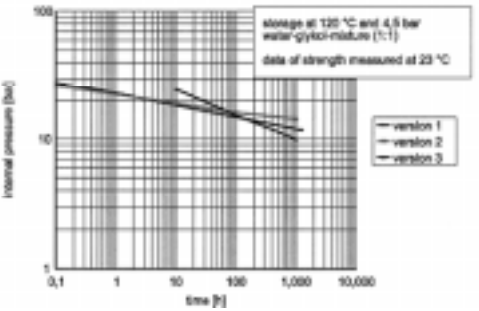

Figure 7. Internal pressure strength for describing the damage.

effects a comparable damaging of the product as it will be caused by the influence of the time-temperature-profile for the demanded lifetime.

The example described in the following explains this principle and shows at the same time the measurement of a suitable indicator-property for products loaded with an internal pressure.

For this product which is predominated loaded with a temperature, a medium and an internal pressure the time-temperature-profile is shown in Figure 5. With equation 1 it can be determined that with assumption of a maximum temperature of 130°C for the total life-time, a testing time of about 300,000 hours at a testing temperature of 120°C results. By taking into consideration a maximum temperature of 82°C the result is 720 hours which is still a long testing time. With the principle of estimation of time-temperature-collectives as described above the testing time can be reduced to 107 hours at a testing temperature of 120°C.

Thereby the separate time-temperature-intervals are separately inspected. For each interval a testing time at testing temperature can be estimated with Arrhenius. With the described procedure the ageing progress can be estimated.

The addition of these ageing progresses is the real damaging caused by the time-temperature-profile. The percentages of time and ageing evaluated with this principle are shown in Figure 6. By this it can be illustrated that especially the high temperatures are very critical and that they cause a high percentage of ageing although they effect only for a short time. Because of this it is obvious that a dimensioning with this maximum temperature for the whole lifetime leads to a large over-dimensioning of the product. The characteristic product value to describe the damaging of the product caused by the ageing progress of the material is measured with a so-called "bursting test". This means that the parts are tested with a raising internal pressure up to a failure. The bursting strength is an indicator for damage. A cor-

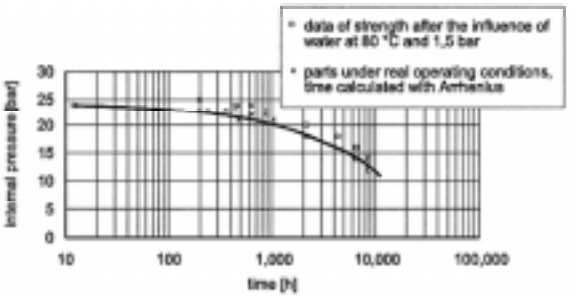

Figure 8. Comparison between calculated and measured damaging.

responding pressure-time-curve for this internal pressure strength is given in Figure 7 for the examined product.

For examination of the above described theory such as pressure-time-curve was measured for a special product. A few parts of this product are operating under real conditions for a determined time. The internal pressure strength of these parts can be compared with the measured values of testing (Figure 8). The operating time can be converted with the statement of Arrhenius and so these results can be compared with the results of the product tests.

The results of this comparison illustrate that the parts under the real operating conditions show a higher internal pressure strength than evaluated with the described theory. This shows that the estimation of time-temperature-collectives is an estimation to the secure side. On the other hand with this theory a large over-dimensioning can be avoided.